Research in Astronomy and Astrophysics, 24:035014 (11pp), 2024 March https://doi.org/10.1088/1674-4527/ad21d5

The Influence of Velocity-dependent Correction Factor on Proton Decay Reactions in Massive White Dwarfs

Jing-Jing Liu and Dong-Mei Liu
College of Science, Hainan Tropical Ocean University, Sanya 572022, China; liujingjing68@126.com
Received 2023 November 6; revised 2024 January 11; accepted 2024 January 22; published 2024 March 4

Abstract

Twenty-five typical massive white dwarfs (WDs) are selected and the proton decay reaction catalyzed by magnetic monopoles (MMs) for these WDs is discussed. A velocity-dependent correction factor strongly affects the cross-section. We find that a strong suppression controls the monopole catalysis of nucleon decay by the correction factor. The maximum number of MMs is captured and the luminosity can be 2.235×10^{21} and 1.7859×10^{32}erg s^{-1} (e.g., for the O+Ne core mass WD J055631.17+130639.78). The luminosities of most massive WDs agree well with the observations at relatively low temperatures (e.g., $T_6 = 0.1$), but can be three and two orders of magnitude higher than those of the observations for model (I) and (II) at relatively high temperatures (e.g., $T_6 = 10$), respectively. The luminosities of model (I) are about one order of magnitude higher than those of model (II). Since we consider the effect of the number of MMs captured on the mass–radius relation and the suppression of the proton decay by the correction factor, the study by model (II) may be an improved estimation.

Key words: astroparticle physics – nuclear reactions – nucleosynthesis – abundances – (stars:) white dwarfs

1. Introduction

White dwarfs (WDs) form at very high temperatures. Their radiation decreases over time from the initial high color temperature to turn red. Some observations show that the effective temperature of WDs may be mostly between 5500 K - 40000 K (e.g., Gao et al. 2023), and a few are outside this range, and the total thermal energy may be less than 10^{47} erg. What are the specific heat sources in WDs? What can provide this energy to WDs? These issues will be discussed in this paper.

From the Stefan-Boltzmann law, the radiation energy luminosity is defined by the surface effective temperature $T_{\rm eff}$,

$$L_{\rm rad} = 4\pi R^2 \sigma T_{\rm eff}^4, \quad (1)$$

where $L_{\rm rad}$ and R are the radiation luminosity and radius of the WD respectively. $\sigma = 5.6704 \times 10^{-5}$ erg s^{-1} cm^{-2} K^{-4} is the radiation constant.

Mestel (1952), Avakian (1972) and Bildsten & Hall (2001) investigated the problem of WD energy sources. Their results showed that small amounts of ^{22}Ne in WDs may be an extra source of heat. A possible heat source may be considered from ^{22}Ne sedimentation (e.g., Deloye & Bildsten 2002; Garcła-Berro et al. 2008). Lobato et al. (2018) and Cheng et al. (2019) also discuss the cooling anomaly of high-mass WDs. They pointed out that this problem is from ^{22}Ne. By using molecular dynamics methods and phase diagrams, Caplan et al. (2020) stated that ^{22}Ne cannot be a possible cause of the heating in WDs.

In this paper, we present a new method to solve the energy source problem for 25 typical massive WDs selected from Kilic et al. (2021). Our model is based on the magnetic monopole (hereafter MM) catalytic proton decay (RC effect) (e.g., Rubakov 1981; Callan 1983). Issues related to MMs are forefront subjects in astrophysics (e.g., Detrixhe et al. 2011; Rajantie 2012; Fujii & Pierre 2015; Frank et al. 2019; Kain 2019). We studied the problem of MMs and other related issues (e.g., Peng et al. 2017, 2020; Liu 2013, 2014; Liu & Gu 2016a; Liu & Liu 2017c, 2018a; Liu 2016b; Liu & Liu 2016c; Liu 2016d; Liu et al. 2017a, 2017b; Liu & Liu 2018b). Some scholars also discussed other energy mechanisms of WDs, such as magnetic field evolution, the state equation of the WDs and related issues (e.g., Deng et al. 2020, 2021; Li et al. 2016; Li & Gao 2023; Li et al. 2023; Fu et al. 2020; Gao et al. 2016, 2017, 2019, 2023; Dong et al. 2023; Wang et al. 2020; Yan et al. 2021; Zhu et al. 2016). Their researches provide a database for further exploration of the evolution of WDs. Recently, the energy source problem for WDs has been discussed by Peng & Liu (2023); Liu et al. (2023a, 2023b); Liu & Liu (2023c) and Liu & Liu 2023d). However, the influence of the velocity-dependent correction factor on the cross-sections in the Rubakov process is ignored in the above works. Because the velocity-dependent correction factor strongly affects the proton decay thermonuclear reactions, we re-examine this issue in this paper.

The plan of this paper is given as follows. In the next section, we present our recent works on the number of possible MMs, and the luminosity by MM catalytic proton decay. The MM model and the RC luminosity in WDs are shown in Section 3. Results and discussions are given in Section 4. Section 5 summarizes some conclusions.

2. Our Recent Works on the Numbers of MMs Captured and the Luminosity by Catalytic Proton Decay in Stars

Recently, we discussed the energy source problem for WDs. First, we discussed the numbers of MMs captured in space at the surface of stars, which is given by (Peng et al. 1985; Peng & Liu 2023; Liu et al. 2023a, 2023b; Liu & Liu 2023c, 2023d)

$$N_{m(\mathrm{sur})} = 5.7 \times 10^{-25} m_9 v_{-3} n_{\mathrm{B}}^0 \frac{\zeta_m^0}{\zeta_s}, \tag{2}$$

where v_m is the velocity of the MMs in space, $v_{-3} = v_m/10^{-3}c$, $m_9 = m_m/10^9 m_p$, $10^3 m_p \leqslant m_m \leqslant 10^{16} m_p$, c is the speed of light and ζ_m^0 is the amount of MMs in space. The superscript (0) denotes space. $n_{\mathrm{B}}^0 = (10^4$–$10^6)\,\mathrm{cm}^{-3}$ is the number density of baryons in the space of the Milky Way (Peng et al. 1985) and the Newton saturation value ζ_s is the maximum number of MMs, which is defined as $\zeta_s = G m_B m_m / g_m^2 \approx 1.9 \times 10^{-32} \frac{m_m}{10^9 m_p}$. $g_m = 3hc/2e$ and m_B, which are the magnetic charge of MMs and the baryon number mass, respectively. The MM mass is about $m_m \sim 10^{16} m_p$ (Polyakov 1974), where m_p is the mass of a proton.

The total number of MMs trapped in space after the formation of stars (or planets) is estimated as

$$\begin{aligned} N_{m(\mathrm{tot})} &= 4\pi R^2 t N_{m(\mathrm{sur})} \\ &= 3.463 \times 10^7 v_{-3} n_{\mathrm{B}}^0 t_9 m_9 \left(\frac{\zeta_m^0}{\zeta_s}\right)\left(\frac{R}{R_\odot}\right)^2 \\ &= 3.463 \times 10^7 \xi v_{-3} n_{\mathrm{B}}^0 t_9 R_*^2, \end{aligned} \tag{3}$$

where $R_* = R/R_\odot$, $t_9 = t/10^9$ yr and $\xi = m_9 F/\zeta_s$. R, t and F are the radius, age of the star and MM flux in space, respectively.

The reactions $pM \rightarrow e^+\pi^0 M + \mathrm{debris}(85\%)$, and $pM \rightarrow e^+\mu^\pm M + \mathrm{debris}(15\%)$ are named proton decay reactions catalyzed by MMs, which were proposed by the RC effect. The luminosity due to the RC effect is (Peng et al. 1985; Peng & Liu 2023; Liu et al. 2023a, 2023b; Liu & Liu 2023c, 2023d)

$$L_m \approx \frac{4\pi}{3} r_c^3 n_m n_{\mathrm{B}} \langle \sigma_m v_{\mathrm{T}} \rangle m_{\mathrm{B}} c^2 = N_m n_B \langle \sigma_m v_{\mathrm{T}} \rangle m_{\mathrm{B}} c^2, \tag{4}$$

where r_c, n_m and n_B are the radius of the stellar central region, and the number density of MMs and nucleons, respectively. The reaction cross-section of the RC effect is about $\sigma_m \approx 10^{-25} \sim 10^{-26}\,\mathrm{cm}^2$. $1 m_{\mathrm{B}} c^2 \approx 1\mathrm{GeV} \approx 1.6 \times 10^{-3}$ erg s. v_{T} is the thermal movement speed of the nucleus relative to the MM, and $v_{\mathrm{T}} = \sqrt{kT/m_B} \approx 8.691 \times 10^3 T^{1/2}$ cm/s, where T is the temperature, k is the Boltzmann constant and $m_B \approx 1.78 \times 10^{-24}$g is the nucleon mass. The number density of nucleons can be written as

$$n_B = 2.90 \times 10^{16} \left(\frac{R}{R_g}\right)^{-3} (M_{12})^{-2} = 2.242 \times 10^{24} M_* R_*^{-3}\ \mathrm{cm}^{-3}, \tag{5}$$

where $R_g = 2.96 \times 10^5 M_*$ is the Schwarzschild radius, and $M_{12} = M_*/10^{12}$, $M_* = M/M_\odot$ and $R_* = R/R_\odot$ (Peng et al. 1985; Peng & Liu 2023; Liu et al. 2023a, 2023b; Liu & Liu 2023c, 2023d).

As a general rule, the values of reaction cross-section are distributed between 10^{-26} and $10^{-24}\,\mathrm{cm}^2$. Ma & Tang (1983) gave an estimation of $\sigma_m \approx 4.28676 \times 10^{-24}\,\mathrm{cm}^2$ by using the SU(5) Grand Unified Theory (GUT).

3. The MM Model and RC Luminosity in WDs

3.1. MM Catalytic Proton Decay Model (I) in WDs

The mass–radius relation of WDs is one of the interesting issues for astrophysicists. For zero-temperature stars, the equations of hydrostatic equilibrium and mass conservation are given by (Cox & Giuli 1968)

$$\frac{dP}{dr} = -\frac{G m_r \rho}{r^2}, \tag{6}$$

$$\frac{dM}{dr} = 4\pi r^2 \rho, \tag{7}$$

where r is the radial variable (when $r = 0$ at the center) and m_r is the mass inside a sphere of radius r.

According to Equations (6)–(7), the mass–radius relation can be expressed as the following

$$R_* \approx \frac{P_0}{R_\odot G (\rho_0 \mu_e)^{5/3}} M^{-1/3} = 1.080 \times 10^{-2} \mu_e^{-5/3} M_*^{-1/3}, \tag{8}$$

where $P_0 = \pi m^4 c^5/(3h^3) \approx 5.9637 \times 10^{22}\,\mathrm{dyn/cm}^2$, $\mu_e = A/Z$ is the molecular weight per electron, $\rho_0 = n_0 u \approx 9.6838 \times 10^5 \mathrm{g/cm}^3$, $n_0 = 8\pi m^3 c^3/(3h^3) \approx 5.8336 \times 10^{29}\,\mathrm{cm}^{-3}$ and u is an atomic mass unit. According to Equations (5) and (8) we have

$$n_B^* = 2.242 \times 10^{24} M_* (R_*^0)^{-3} = 1.7794 \times 10^{30} \mu_e^5 M_*^2\ \mathrm{cm}^{-3}. \tag{9}$$

According to Equations (3) and (9), in the case without considering the RC effect on the mass–radius relation, we can estimate the number of MMs captured from space in the lifetime of the WD's progenitor star as

$$N_1 = N_{m(\mathrm{tot})}(\mathrm{I}) = 3.463 \times 10^7 \xi v_{-3} n_{\mathrm{B}}^0 t_9 (R_*^0)^2. \tag{10}$$

According to Equations (4) and (8)–(10) in the case without considering the RC effect on the relation of mass–radius, the

total luminosity due to the nuclear decay reaction catalyzed by MMs is given by

$$L_m(\mathrm{I}) \approx \frac{4\pi}{3} r_c^3 n_m n_{\mathrm{B}}^* \langle \sigma_m v_{\mathrm{T}} \rangle m_{\mathrm{B}} c^2 = N_2 n_B^* \langle \sigma_m v_{\mathrm{T}} \rangle m_{\mathrm{B}} c^2 = 5.541 \times 10^4 n_B^* v_{-3} n_{\mathrm{B}}^0 \langle \sigma_m v_{\mathrm{T}} \rangle \xi t_9 (R_*^0)^2. \quad (11)$$

3.2. MM Catalytic Nuclear Decay Model (II) in WDs

When only the RC effect is considered as an energy release process, the equation of state in WDs can be obtained by Izawa (1986)

$$\frac{\partial P}{\partial M(\mathrm{r})} = -\frac{GM(\mathrm{r})}{4\pi r^4}, \quad (12)$$

$$\frac{\partial L_{\mathrm{r}}}{\partial M(\mathrm{r})} = \varepsilon_{\mathrm{m}}, \quad (13)$$

$$\frac{\partial M(\mathrm{r})}{\partial r} = 4\pi r^2 \rho, \quad (14)$$

where ε_{m} is the energy generation rate per unit mass resulting from mass annihilation.

According to Equations (12)–(14), the mass–radius relation is determined by Izawa (1986)

$$R_*^{\mathrm{MR}} \approx 2 \times 10^{-10} \left(\frac{M}{M_\odot} \right)^{-2.35} N_2^{0.45} = 2 \times 10^{-10} M_*^{-2.35} N_2^{0.45}. \quad (15)$$

From the number of MMs captured and the RC effect for some low-mass WDs, the number of MMs captured in WDs is given as

$$N_2 = N_{m(\mathrm{tot})}^{\mathrm{MR}}(\mathrm{II}) = 3.463 \times 10^7 \xi v_{-3} n_{\mathrm{B}}^0 t_9 (R_*^{\mathrm{MR}})^2. \quad (16)$$

According to Equations (5) and (15) we have

$$n_B^{\mathrm{MR}} = 2.242 \times 10^{24} M_* (R_*^{\mathrm{MR}})^{-3} = 2.803 \times 10^{53} N_2^{-1.35} M_*^{8.05}\ \mathrm{cm}^{-3}. \quad (17)$$

According to Equations (4) and (15)–(17), in the case that considers the RC effect and the correction factor effect, the cross-section of the RC effect is corrected, and the total luminosity is expressed as

$$L_m^{\mathrm{MR}}(\mathrm{II}) \approx \frac{4\pi}{3} r_c^3 C n_m n_{\mathrm{B}}^{\mathrm{MR}} \langle \sigma_m v_{\mathrm{T}} \rangle m_{\mathrm{B}} c^2 = C N_m^{\mathrm{MR}} n_B^{\mathrm{MR}} \langle \sigma_m v_{\mathrm{T}} \rangle m_{\mathrm{B}} c^2 = 5.541 \times 10^4 n_B^{\mathrm{MR}} v_{-3} C n_{\mathrm{B}}^0 \langle \sigma_m v_{\mathrm{T}} \rangle \xi t_9 (R_*^{\mathrm{MR}})^2. \quad (18)$$

In Equation (18), C is the factor describing the correction effect, which may correct the cross-section of the RC effect. Due to an extra angular momentum carried by the monopole electric charge system, Arafune & Fukugita (1983) discussed a velocity-dependent correction factor, which will strongly affect the cross-section because of the RC effect. The correction factor is given by

$$C = \left(\frac{\beta}{\beta_0} \right)^{\nu} = (\beta r_0 m_N A^{4/3})^{\nu}, \quad (19)$$

where $\beta = v_m/c$, $\beta_0 = 1/(r_0 m_N A^{4/3})$, $r_0 = 1.2$ fm and m_N and A are the neutron mass and nuclear mass number, respectively. In the monopole-electric charge system, $\nu = -\frac{1}{2} + \left(\frac{1}{4} + |q|\right)^{1/2}$, $q = Z \times (\pm\frac{1}{2}, \pm 1, \ldots)$.

4. Results and Discussions

Study of the MM flux has gained considerable interest issue in the astrophysical fields since GUTs predicted baryon decay reaction and the existence of the MMs (G't 1974; Parker 1970). Parker (1970) gave the MM flux as $F \leqslant 10^{-16}\,\mathrm{cm}^{-2}\mathrm{s}^{-1}\mathrm{sr}^{-1}$ (Parker 1970). A limit on the flux and the catalysis cross-section in neutron stars may be $F(\sigma v)_{-28} \leqslant 10^{-21}\mathrm{cm}^{-2}\mathrm{s}^{-1}\mathrm{sr}^{-1}$ (Kolb & Turner 1984). Freese (1984) estimated the MM flux in WDs, which may be $F(\sigma v)_{-28} \leqslant 10^{-18}\,\mathrm{cm}^{-2}\,\mathrm{s}^{-1}\,\mathrm{sr}^{-1}$. Freese & Krasteva (1999) also showed that the bound was stated as $F(\sigma v)_{-28} \leqslant 10^{-28}\,\mathrm{cm}^{-2}\,\mathrm{s}^{-1}\,\mathrm{sr}^{-1}$. In this paper, we select some typical parameters as follows: the number density of baryons $n_B^0 = 10^5\,\mathrm{cm}^{-3}$ and the temperature $T_6 = 0.01, 0.1, 1, 10$. The mass of MM is selected as $m_{16} = 10\,\mathrm{GeV}$, and the MM flux is $F = 1.9 \times 10^{-23}\,\mathrm{cm}^{-2}\mathrm{s}^{-1}\mathrm{sr}^{-1}$. According to the relation $\xi = m_9 F/\zeta_s$, we have $\xi = 10^3$.

Figure 1 shows the correction factor as a function of the mass of MM for some typical nuclei due to the RC effect. One finds that as the mass of MM increases, the correction factor decreases. For example, when $m_{16} = 90$ GeV, the correction factors of ^{4}He, ^{12}C, ^{16}O, ^{28}Si, ^{40}Ar, ^{40}Ca and ^{56}Fe can be calculated as 6.902×10^{-2}, 4.022×10^{-4}, 2.803×10^{-4}, 2.699×10^{-4}, 8.207×10^{-4}, 5.239×10^{-4} and 2.519×10^{-3}, respectively. These results show that a strong suppression controls the monopole catalysis of nucleon decay. Due to the effect of these correction factors, the cross-section for the Rubakov process also receives a strong suppression. This suppression is caused by a long range force, which originates from an extra angular momentum carried by a monopole-electric-charge system (i.e., $q = Z \times (\pm\frac{1}{2}, \pm 1, \ldots)$ with Z the charge of the nucleus, e.g., Arafune & Fukugita 1983). For example, for some heavy elements more important suppression arises from a strong repulsive force against a slowly moving MM because of the Zeeman effect and the diamagnetic effect on the atomic electrons (e.g., Malkus 1951). Even in the case of light atoms of helium, the repulsive potential is very small (e.g., it is about 16 keV for helium).

Figure 2 shows the number of MMs captured from space in the lifetime of the O+Ne core (panels (a)-(d)) and C+O core ((e)∼(f)) high-mass WDs (Kilic et al. 2021) for model (I) and (II) as a function of M_* due to the RC effect when $\xi = 10^2$ and $n_B^0 = 10^6\,\mathrm{cm}^{-3}$ at the temperature of $T_6 = 0.01, 0.1, 1, 10,$

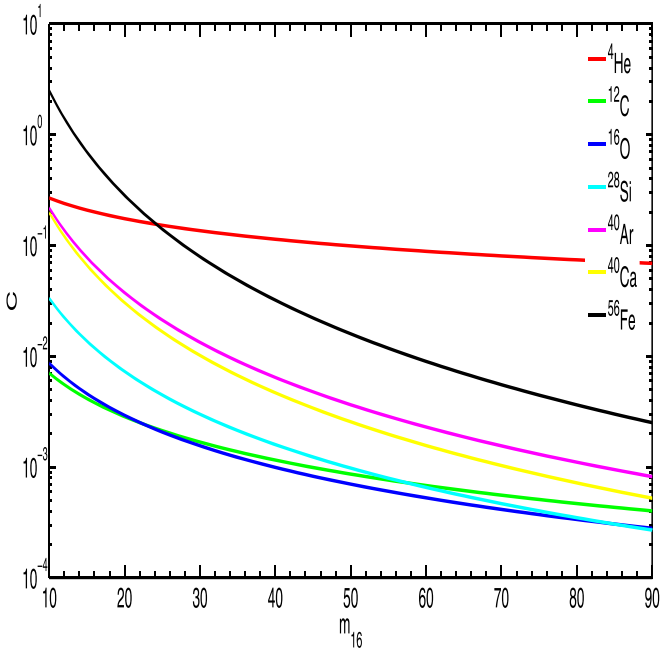

Figure 1. The correction factor as a function of m_{16} for some typical nuclei. Here $m_{16} = m_m/10^{16}$ GeV is the mass of MM.

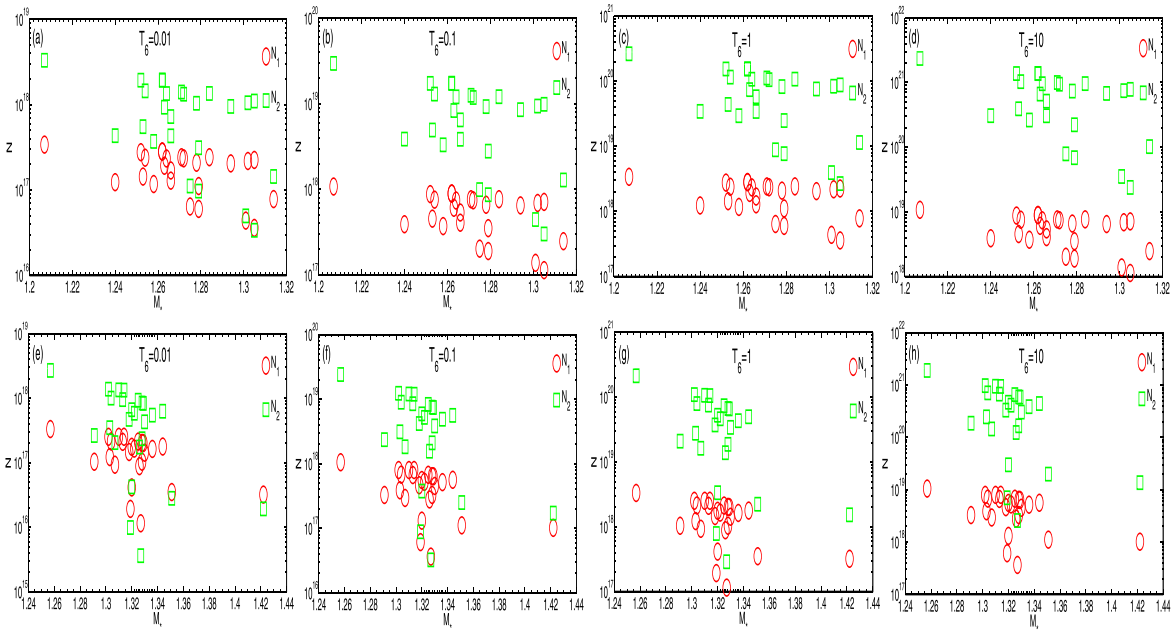

Figure 2. The number of MMs captured from space in the lifetime of the O+Ne core high-mass WDs ((a)-(d)) and the C+O core high-mass WDs ((e)-(h)) (Kilic et al. 2021) for model (I) and (II) as a function of M_* when $\xi = 10^2$ and $n_B^0 = 10^6\,\mathrm{cm}^{-3}$ at the temperature of $T_6 = 0.01$, 0.1, 1, 10, respectively.

respectively. As the temperature increases, the number of MMs captured increases by about two and three orders of magnitude for model (I) and model (II), respectively. For example, for model (I) in panels (a)-(d), the number of MMs captured increases by about two orders of magnitude. (i.e., it first increases from 3.410×10^{17} to 1.078×10^{18}, then increases from 3.410×10^{18} to 1.078×10^{19}) for WD J055631.17 +130639.78 ($M_* = 1.207$, $T_{eff} = 8340$ K, $t_9 = 3.33$) when the

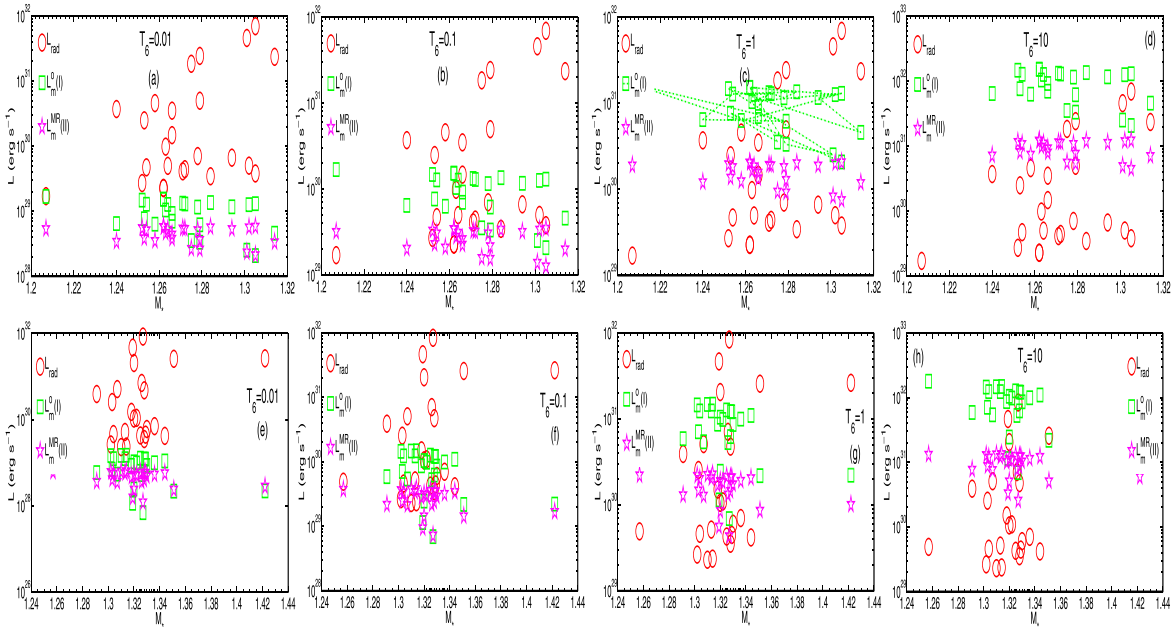

Figure 3. The luminosity as a function of M_* for the O+Ne core high-mass WDs ((a)-(d)) and the C+O core high-mass WDs ((e)-(h)) (Kilic et al. 2021) when $m_{16} = 10$ GeV, $C = 7.037 \times 10^{-3}$, $\xi = 10^3$ and $n_B^0 = 10^6$ cm^{-3} at the temperature of $T_6 = 0.01$, 0.1, 1, 10, respectively.

temperature increases from $T_9 = 0.01$ to $T_6 = 10$. However, the number of MMs captured increases by about three orders of magnitude for model (II) (i.e., it increases from 3.322×10^{18} to 2.352×10^{21}).

When the temperature is certain, one sees that the number of MMs captured $N_2 > N_1$. The higher the mass is, the larger the number of MMs captured becomes from Figure 2. For example, the maximum MMs captured are $N_1 = 1.078 \times 10^{19}$ and $N_2 = 2.352 \times 10^{21}$, for the O+Ne core high-mass WD J055631.17+130639.78 for model (I) and (II) at $T_6 = 10$, respectively. However, the maximum MMs captured are $N_1 = 1.053 \times 10^{19}$ and $N_2 = 1.907 \times 10^{21}$, for C+O core high-mass WD J055631.17+130639.78. On the one hand, by comparing the number of MMs captured of low-mass C+O core WD J055631.17+130639.78 with that of high-mass C+O core WD J190132.74+145807.18, one can find that the number of MMs captured of WD J055631.17+130639.78 is $N_1 = 1.053 \times 10^{19}$, which is larger than that of WD J190132.74 +145807.18 (i.e., $N_1 = 1.016 \times 10^{18}$) for model (I). Under the same condition, we can see from Figure 2 that the numbers of MMs captured are $N_1 = 1.907 \times 10^{21}$ and $N_1 = 1.365 \times 10^{19}$ for WD J055631.17+130639.78 and WD J190132.74 +145807.18, respectively for model (II) at $T_6 = 10$. The main reason is that according to Equations (8) (10), (15) and (16), we have $N_{1,2} \propto 1/M_*$, but $N_{1,2} \propto T_6$. On the other hand, the effect of mass–radius on MMs captured is ignored for model (I). Model (II) considers the effect of mass–radius and the RC effect on the number of MMs captured, so the data are relatively accurate.

The mass–radius relation in model (I) is considered only on the condition of zero temperature according to classical formula Equation (8). According to Equation (15), the mass–radius relation in model (II) is considered on the condition of zero temperature, as well as the RC effect and the number of MMs captured N_2 only for some lower mass WDs. It is found that, if a star contains a sufficient number of monopoles, its radius increases after some stages and finally it dissolves into a diffuse state. However, its lifetime is much longer than the age of the universe because an energy source is rest mass, which is much larger than the nuclear energy.

From Figure 1, when $m_{16} = 10$ GeV, the correction factors of ^{12}C and ^{16}O can be 7.037×10^{-3}, and 8.663×10^{-3}, respectively. However, the correction factors can be 6.821×10^{-4} and 5.279×10^{-4} when $m_{16} = 60$ GeV. In this paper, we select $m_{16} = 10$ GeV and the correction factor $C = 7.037 \times 10^{-3}$ for our WD samples (Kilic et al. 2021). Figure 3 displays the luminosities as a function of M_* for WDs (Kilic et al. 2021) at the temperature of $T_6 = 0.01$, 0.1, 1, 10 when $m_{16} = 10$ GeV, $C = 7.037 \times 10^{-3}$ and $\xi = 10^3$, $n_B^0 = 10^6$ cm^{-3}. One sees that the luminosities for WDs increase as the temperature increases for model (I) and (II), but decrease for model (II). For example, from Figure 3 for model (I), luminosities increase from 1.687×10^{29} to 1.687×10^{32}, for WD J055631.17+130639.78 when the temperature increases from $T_9 = 0.01$ to $T_6 = 10$, and increase from 5.404×10^{28} to 1.142×10^{31} for model (II). To compare the luminosities of model (I) with those of model (II), one can see that the luminosities of model (I) agree well with those of

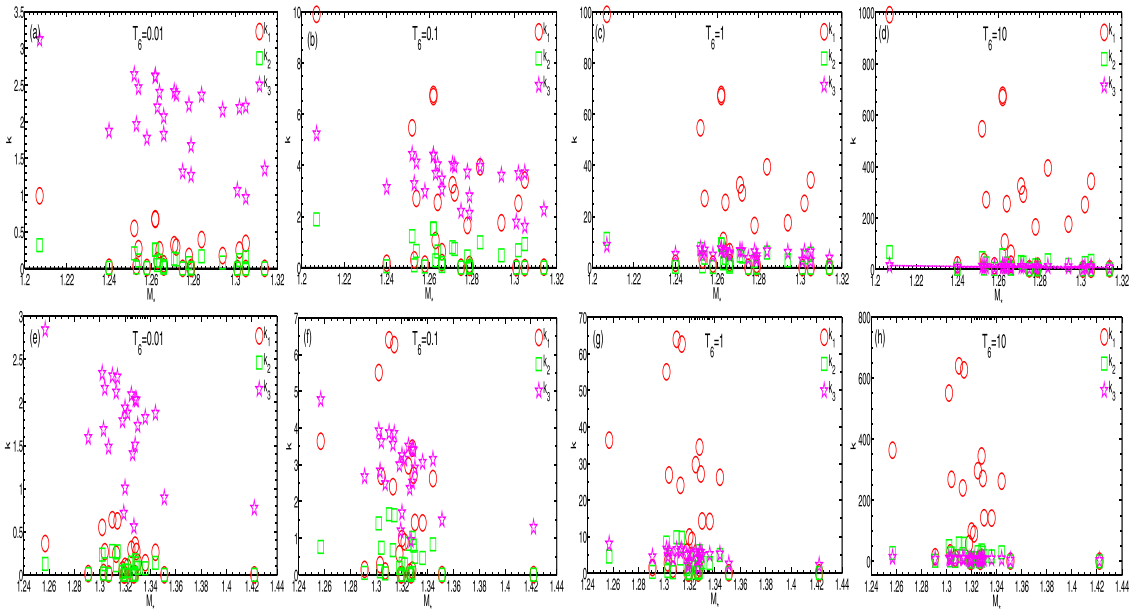

Figure 4. The scaling factor ($k_1 = L_m^0(\mathrm{I})/L_{\mathrm{rad}}$; $k_2 = L_m^{\mathrm{MR}}(\mathrm{II})/L_{\mathrm{rad}}$; $k_3 = L_m(\mathrm{I})/L_m^{\mathrm{MR}}(\mathrm{II})$) as a function of M_* for the O+Ne core high-mass WDs ((a)-(d)) and the C +O core high-mass WDs ((e)-(h)) (Kilic et al. 2021) when $m_{16} = 10$ GeV, $C = 7.037 \times 10^{-3}$, $\xi = 10^3$ and $n_B^0 = 10^6$ cm^{-3} at the temperature of $T_6 = 0.01$, 0.1, 1, 10, respectively.

Table 1

Some Information on the High-mass WD Model (Kilic et al. 2021). All solutions above 1.29 $M_\odot$ for the O+Ne core models and above 1.334 $M_\odot$ for the C+O core models are extrapolated

Star	Star Name	Composition	T_{eff} (K)	O+Ne core Mass ($M_\odot$)	O+Ne core Cooling Age (Gyr)	C+O core Mass ($M_\odot$)	C+O core Cooling Age (Gyr)
1	J010338.56−052251.96	H	9040 ± 70	1.262 ± 0.003	2.84 ± 0.03	1.310 ± 0.003	2.60 ± 0.04
2	J025431.45+301935.38	logH/He = − 5	11060 ± 560	1.302 ± 0.024	2.25 ± 0.10	1.330 ± 0.016	1.49 ± 0.17
3	J114012.81+232204.7	H	11 860 ± 220	1.294 ± 0.008	2.10 ± 0.04	1.336 ± 0.006	1.71 ± 0.06
4	J132926.04+254936.4	H	29 010 ± 750	1.314 ± 0.006	0.81 ± 0.05	1.351 ± 0.006	0.37 ± 0.03
5	J172736.28+383116.9	H	9420 ± 200	1.252 ± 0.012	2.78 ± 0.08	1.302 ± 0.011	2.59 ± 0.12
6	J183202.83+085636.24	He	34 210 ± 1020	1.301 ± 0.006	0.45 ± 0.03	1.319 ± 0.004	0.20 ± 0.02
7	J190132.74+145807.18	H	29 100 ± 480	1.279 ± 0.003	0.61 ± 0.02	1.319 ± 0.004	0.35 ± 0.02
8	J221141.80+113604.5	H	9020 ± 160	1.262 ± 0.009	2.85 ± 0.07	1.310 ± 0.008	2.61 ± 0.11
9	J225513.48+071000.9	H	10 990 ± 210	1.252 ± 0.012	2.36 ± 0.05	1.302 ± 0.011	2.18 ± 0.09
10	J235232.30−025309.2	H	10 680 ± 100	1.272 ± 0.003	2.38 ± 0.02	1.319 ± 0.003	2.10 ± 0.03
11	J004917.14−252556.81	H	13 020 ± 460	1.263 ± 0.011	1.94 ± 0.08	1.312 ± 0.010	1.72 ± 0.09
12	J032900.79−212309.24	H	10 330 ± 290	1.305 ± 0.010	2.32 ± 0.06	1.344 ± 0.008	1.87 ± 0.09
13	J042642.02−502555.21	H	17 900 ± 1570	1.264 ± 0.019	1.30 ± 0.16	1.312 ± 0.016	1.08 ± 0.16
14	J043952.72+454302.81	H	19 120 ± 630	1.258 ± 0.008	1.18 ± 0.06	1.307 ± 0.007	0.96 ± 0.06
15	J055631.17+130639.78	H	8340 ± 260	1.207 ± 0.021	3.33 ± 0.12	1.257 ± 0.023	3.34 ± 0.18
16	J060853.60−451533.03	H	19 580 ± 1910	1.258 ± 0.021	1.13 ± 0.16	1.307 ± 0.019	0.92 ± 0.17
17	J070753.00+561200.25	H	18 100 ± 350	1.240 ± 0.005	1.23 ± 0.04	1.291 ± 0.005	1.06 ± 0.04
18	J080502.93−170216.57	H	10 830 ± 110	1.254 ± 0.004	2.40 ± 0.03	1.304 ± 0.003	2.20 ± 0.03
19	J093430.71−762614.48	H	10 050 ± 1350	1.284 ± 0.055	2.47 ± 0.35	1.328 ± 0.047	2.11 ± 0.50
20	J095933.33−182824.16	H	12 000 ± 180	1.273 ± 0.005	2.12 ± 0.03	1.320 ± 0.004	1.83 ± 0.04
21	J111646.44−160329.42	H	10 480 ± 170	1.264 ± 0.007	2.45 ± 0.05	1.312 ± 0.006	2.21 ± 0.07
22	J125428.86−045227.48	H	14 420 ± 390	1.258 ± 0.008	1.71 ± 0.06	1.308 ± 0.007	1.52 ± 0.06
23	J174441.56−203549.05	H	27 140 ± 890	1.271 ± 0.008	0.65 ± 0.06	1.312 ± 0.008	0.43 ± 0.04
24	J180001.21+451724.7	H	16 410 ± 290	1.253 ± 0.003	1.44 ± 0.03	1.303 ± 0.004	1.26 ± 0.04
25	J181913.36−120856.44	H	37 970 ± 1940	1.305 ± 0.009	0.37 ± 0.03	1.327 ± 0.006	0.12 ± 0.03

Table 2

The Comparisons Among Several Luminosities Due to the RC Effect for the O+Ne Core High Mass WD model (Kilic et al. 2021) at Relatively Low Temperature $T_6 = 0.1$, in which the Parameters $1.207 \leqslant M_* \leqslant 1.315$, $m_{16} = 10$ GeV, $C = 7.037 \times 10^{-3}$, $\xi = 10^3$ and $n_B^0 = 10^6$ cm^{-3} (note $k_1 = L_m(\mathrm{I})/L_{\rm rad}$, $k_2 = L_m^{\rm MR}(\mathrm{II})/L_{\rm rad}$, and $k_3 = L_m(\mathrm{I})/L_m^{\rm MR}(\mathrm{II})$)

Star	M_*	$T_{\rm eff}$	t_9	N_1	N_2	$L_{\rm rad}$	L_m(I)	$L_m^{\rm MR}$(II)	k_1	k_2	k_3
1	1.262	9040	2.84	8.9280e16	1.7278e19	2.2800e29	1.5266e30	3.4703e29	6.6926	1.5214	4.3991
2	1.302	11060	2.25	6.9280e16	9.4080e18	5.0100e29	1.2608e30	3.4214e29	2.5189	0.6835	3.6852
3	1.294	11860	2.10	6.4920e16	8.5206e18	6.6500e29	1.1672e30	3.2207e29	1.7562	0.4846	3.6239
4	1.314	29010	0.81	2.4790e16	1.2860e18	2.3548e31	4.5950e29	2.0170e29	0.0195	0.0086	2.2780
5	1.252	9420	2.78	8.7860e16	1.7305e19	2.7000e29	1.4786e30	3.3316e29	5.4687	1.2322	4.4381
6	1.310	34210	0.45	1.3860e16	4.4400e17	4.5842e31	2.5190e29	1.4078e29	0.0055	0.0031	1.7893
7	1.279	29100	0.61	1.9010e16	8.6600e17	2.4275e31	3.3380e29	1.5638e29	0.0138	0.0064	2.1345
8	1.262	9020	2.85	8.9600e16	1.7393e19	2.2600e29	1.5320e30	3.4770e29	6.7759	1.5379	4.4060
9	1.264	10990	2.36	7.4110e16	1.2052e19	4.9800e29	1.2713e30	3.1525e29	2.5542	0.6334	4.0326
10	1.272	10680	2.38	7.4430e16	1.1844e19	4.4200e29	1.2929e30	3.2409e29	2.9248	0.7332	3.9892
11	1.263	13020	1.94	6.0960e16	8.3400e18	9.8100e29	1.0439e30	2.8222e29	1.0641	0.2877	3.6990
12	1.315	10330	2.32	7.1320e16	9.8510e18	3.8000e29	1.3041e30	3.5089e29	3.4288	0.9226	3.7165
13	1.266	17900	1.30	4.0780e16	3.8490e18	3.4990e30	7.0180e29	2.2842e29	0.2006	0.0653	3.0723
14	1.258	19120	1.18	3.7170e16	3.3120e18	4.5740e30	6.3160e29	2.1161e29	0.1381	0.0463	2.9848
15	1.207	8340	3.33	1.0784e17	2.9607e19	1.7000e29	1.6868e30	3.2192e29	9.9089	1.8911	5.2396
16	1.279	19580	1.13	3.5210e16	2.7940e18	4.9750e30	6.1840e29	2.1951e29	0.1243	0.0441	2.8170
17	1.240	18100	1.23	3.9120e16	3.8680e18	3.7090e30	6.4580e29	2.0541e29	0.1741	0.0554	3.1443
18	1.254	10830	2.40	7.5770e16	1.2978e19	4.7200e29	1.2792e30	3.0908e29	2.7110	0.6550	4.1387
19	1.284	10050	2.47	7.6760e16	1.2093e19	3.4400e29	1.3587e30	3.4231e29	3.9445	0.9938	3.9691
20	1.278	12000	2.12	6.6090e16	9.2730e18	7.0200e29	1.1589e30	3.0938e29	1.6501	0.4405	3.7458
21	1.271	10480	2.45	7.6660e16	1.2567e19	4.1000e29	1.3295e30	3.2836e29	3.2422	0.8008	4.0490
22	1.266	14420	1.71	5.3640e16	6.4800e18	1.4740e30	9.2310e29	2.6559e29	0.6264	0.1802	3.4756
23	1.275	27140	0.65	2.0290e16	9.9300e17	1.8405e31	3.5420e29	1.6010e29	0.0192	0.0087	2.2124
24	1.253	16410	1.44	4.5490e16	4.9380e18	2.4890e30	7.6670e29	2.3270e29	0.3081	0.0935	3.2948
25	1.305	37970	0.37	1.1370e16	3.0100e17	6.9426e31	2.0800e30	1.2784e29	0.0030	0.0018	1.6269

model (II) at the relative temperature (e.g., $T_6 = 0.01$), but as the temperature increases, the difference between the two models becomes bigger and bigger. To compare the luminosities of observation $L_{\rm rad}$ with those of model (I) and model (II), we find that the difference of the luminosities between the observation $L_{\rm rad}$ and our results can be no more than three orders magnitude. For example, for the high mass C+O core WD J190132.74+145807.18, the difference is no more than one order magnitude at $T_6 = 0.01$, but, for the C+O core WD J055631.17+130639.78, the luminosities of the observation $L_{\rm rad}$ are about two and three orders magnitude lower than those of model (II) and (I), respectively.

Figure 4 displays the scaling factor k ($k_1 = L_m(\mathrm{I})/L_{\rm rad}$; $k_2 = L_m^{\rm MR}(\mathrm{II})/L_{\rm rad}$; $k_3 = L_m(\mathrm{I})/L_m^{\rm MR}(\mathrm{II})$) as a function of M_* for the O+Ne(C+O) core WDs (Kilic et al. 2021) when $m_{16} = 10$ GeV, $C = 7.037 \times 10^{-3}$, $\xi = 10^3$ and $n_B^0 = 10^6$ cm^{-3} at the temperatures of $T_6 = 0.01$, 0.1, 1, 10. One can see that model (I) and model (II) agree well with the observations at relatively low temperature (e.g., $T_6 = 0.01$) from Figure 4. As the temperature increases, the difference becomes bigger and bigger. For example, from Figure 4, k_1 increases from 3.121 to 990.9 for the C+O core WD J055631.17+130639.78, but increases from 0.3175 to 67.10. From the value of k_3, the luminosities for model (I) can be only 3.121 times larger than those of model (II), but can be 14.77 times that at $T_6 = 10$ for the C+O core WD J055631.17 +130639.78 from Figure 4(a)–(d). The same conclusions may be obtained from Figure 4(e)–(h).

Tables 1–3 show the comparisons of the luminosities and the scaling factor k due to the RC effect for these high-mass O+Ne core WDs at $T_6 = 0.1$, 10, respectively. The luminosities for most of the O+Ne core WDs for model (I) and model (II) agree well with the observations and the difference among them is no more than one order magnitude at $T_6 = 0.1$. However, as temperature increases (e.g., $T_6 = 10$ in Table 3), the observations can be three and two orders magnitude lower than those of model (I) and model (II), respectively. The scaling factors k_1, k_2 can be in the range of $0.0030 \leqslant k_1 \leqslant 9.9089$ and $0.0018 \leqslant k_2 \leqslant 1.8911$ for the O+Ne core star WD J055631.17+130639.78 and WD J181913.36-120856.44, respectively at $T_6 = 0.1$ in Table 2, but are in the range of $0.2996 \leqslant k_1 \leqslant 990.8927$ and $0.0653 \leqslant k_2 \leqslant 67.1005$ at $T_6 = 10$ in Table 3. Comparing the results from model (I) and model (II), one finds $1.6269 \leqslant k_3 \leqslant 5.2396$ and $4.5851 \leqslant k_3 \leqslant 14.7673$ in Tables 2 and 3, respectively. Table 3 lists 14 WDs, whose values of k_3 exceed a factor of 10 at $T_6 = 10$. For example, the values of k_3 are 12.3983, 10.3862, 10.2135,

Table 3

The Comparisons Among Several Luminosities Due to the RC Effect for the O+Ne Core High-mass WD model (Kilic et al. 2021) at Relatively High Temperature $T_6 = 10$, in Which the Parameters $1.207 \leqslant M_* \leqslant 1.315$, $m_{16} = 10$ GeV, $C = 7.037 \times 10^{-3}$, $\xi = 10^3$ and $n_B^0 = 10^6$ cm^{-3} (note $k_1 = L_m(\mathrm{I})/L_{\rm rad}$, $k_2 = L_m^{\rm MR}(\mathrm{II})/L_{\rm rad}$, and $k_3 = L_m(\mathrm{I})/L_m^{\rm MR}(\mathrm{II})$)

Star	M_*	$T_{\rm eff}$	t_9	N_1	N_2	$L_{\rm rad}$	L_m(I)	$L_m^{\rm MR}$(II)	k_1	k_2	k_3
1	1.262	9040	2.84	8.9280e18	1.3724e21	2.2800e29	1.5266e32	1.2313e31	669.2608	53.9800	12.3983
2	1.302	11060	2.25	6.9280e18	7.4730e20	5.0100e29	1.2608e32	1.2140e31	251.8930	24.2527	10.3862
3	1.294	11860	2.10	6.4920e18	6.7730e20	6.6500e29	1.1672e32	1.1428e31	175.6229	17.1952	10.2135
4	1.314	29010	0.81	2.4790e18	1.0220e20	2.3548e31	4.5950e31	7.1570e30	1.9513	0.3039	6.4204
5	1.252	9420	2.78	8.7860e18	1.3746e21	2.7000e29	1.4786e32	1.1821e31	546.8672	43.7209	12.5082
6	1.310	34210	0.45	1.3806e18	3.5300e19	4.5842e31	2.5190e31	4.9950e30	0.5495	0.1090	5.0430
7	1.279	29100	0.61	1.9001e18	6.8800e19	2.4275e31	3.3380e31	5.5490e30	1.3751	0.2286	6.0160
8	1.262	9020	2.85	8.9600e18	1.3816e21	2.2600e29	1.5320e32	1.2337e31	677.5939	54.5658	12.4179
9	1.264	10990	2.36	7.4110e18	9.5730e20	4.9800e29	1.2713e32	1.1185e31	255.4156	22.4730	11.3654
10	1.272	10680	2.38	7.4430e18	9.4080e20	4.4200e29	1.2929e32	1.1499e31	292.4814	26.0142	11.2431
11	1.263	13020	1.94	6.0960e18	6.6250e20	9.8100e29	1.0439e32	1.0014e31	106.4135	10.2074	10.4252
12	1.315	10330	2.32	7.1320e18	7.8250e20	3.8000e29	1.3041e32	1.2450e31	342.8781	32.7349	10.4744
13	1.266	17900	1.30	4.0780e18	3.0580e20	3.4990e30	7.0180e31	8.1040e30	20.0554	2.3162	8.6588
14	1.258	19120	1.18	3.7170e18	2.6310e20	4.5740e30	6.3160e31	7.5080e30	13.8078	1.6414	8.4122
15	1.207	8340	3.33	1.0784e19	2.3517e21	1.7000e29	1.6868e32	1.1422e31	990.8927	67.1005	14.7673
16	1.279	19580	1.13	3.5210e18	2.2190e20	4.9750e30	6.1840e31	7.7880e30	12.4280	1.5653	7.9395
17	1.240	18100	1.23	3.9120e18	3.7200e20	3.7090e30	6.4508e31	7.2880e30	17.4127	1.9649	8.8618
18	1.254	10830	2.40	7.5770e18	1.0309e21	4.7200e29	1.2792e32	1.0967e31	271.0969	23.2414	11.6644
19	1.284	10050	2.47	7.6760e18	9.6060e20	3.4400e29	1.3587e32	1.2146e31	394.4526	35.2615	11.1865
20	1.278	12000	2.12	6.6090e18	7.3660e20	7.0200e29	1.1589e32	1.0977e31	165.0079	15.6300	10.5571
21	1.271	10480	2.45	7.6660e18	9.9820e20	4.1000e29	1.3295e32	1.1651e31	324.2232	28.4119	11.4115
22	1.266	14420	1.71	5.3640e18	5.1470e20	1.4740e30	9.2310e31	9.4230e30	62.6375	6.3944	9.7956
23	1.275	27140	0.65	2.0290e18	7.8900e19	1.8405e31	3.5420e31	5.6810e30	1.9245	0.3086	6.2355
24	1.253	16410	1.44	4.5490e18	3.9202e20	2.4890e30	7.6670e31	8.2560e30	30.8079	3.3176	9.2861
25	1.305	37970	0.37	1.1370e18	2.3900e19	6.9426e31	2.0800e31	4.5360e30	0.2996	0.0653	4.5851

12.5082, 12.4179, 11.3654, 11.2431, 10.4252, 10.4744, 14.7673, 11.6644, 11.1865, 10.5571 and 11.4115 for the O +Ne core high-mass WD No.1-3, 5, 8-12, 15 and 18-21, respectively.

Tables 4 – 5 also show the comparisons of the luminosities and the scaling factor k for the C+O core WDs at $T_6 = 0.1$, 10. For most of the C+O core WDs, the results of model (I) and model (II) agree well with the observations of $L_{\rm rad}$, and the difference among them is no more than one order of magnitude at $T_6 = 0.1$. However, as the temperature increases (e.g., $T_6 = 10$ in Table 5), the observations of $L_{\rm rad}$ can be three and two orders of magnitude lower than those of model (I) and model (II), respectively. The scaling factors k_1 and k_2 can be in the range of $0.0008 \leqslant k_1 \leqslant 6.4014$ and $0.0009 \leqslant k_2 \leqslant 1.6509$ for the C+O core WD J010338.56-052251.96 and WD J181913.36-120856.44, respectively at $T_6 = 0.1$ in Table 4, but the ranges are $0.0823 \leqslant k_1 \leqslant 640.1393$ and $0.0310 \leqslant k_2 \leqslant 58.5767$ at $T_6 = 10$ in Table 5. From model (I) and model (II), k_3 is in the range of $0.9429 \leqslant k_3 \leqslant 4.7758$ and $2.6575 \leqslant k_3 \leqslant 13.4601$, shown in Tables 4 and 5, for the C +O core WD J055631.17+130639.78 and WD J181913.36-120856.44, respectively.

According to stellar evolution theory, radiative transfer of energy is negligible compared with thermal conduction in the highly degenerate core of WDs, in spite of the reduced opacity of a degenerate gas. It will be shown that the thermal conduction is so great that, during the cooling of a WD, the temperature is always very nearly uniform in the core. MMs trapped inside WDs can catalyze decay of nucleons and provide an additional source of internal heat for the star. An MM which passes through a WD can easily lose enough energy to be captured. Ahlen & Kinoshita (1982) calculated this energy source, which comes from the electronic interactions and is given by $dE/dx \approx 100\rho\beta$ GeV/cm, where ρ is the density of a WD (in g cm^{-3}), and $\beta = v_m/c$ is the ratio of the velocity of the MM to the speed of light as it passes through the WD. Far from the WD, the velocity of a typical MM in the Galaxy is the virial velocity (i.e., $v_m = 10^{-3}c$). When an MM falls into the gravitational potential well of a WD, it is accelerated and β increases to $(v_m^2 + 2GM/R)^{1/2}$ at the surface of the WD. The energy loss in traveling through the WD can be about 5×10^{17} MeV. Once the MM is captured, it sinks toward the center of the WD. If we consider the motion of an MM as a harmonic oscillator with a dE/dX damping term, then the timescale for the MM to fall from rest to the center can be estimated to be about 1000 s.

Based on the above analysis, we can conclude that with the increase in the number of MMs captured by a WD, the

Table 4

The Comparisons Among Several Luminosities Due to the RC Effect for the C+O Core High-mass WD Model (Kilic et al. 2021) at Relatively Low Temperature $T_6 = 0.1$, in which the Parameters $1.257 \leqslant M_* \leqslant 1.422$, $m_{16} = 10$ GeV, $C = 7.037 \times 10^{-3}$, $\xi = 10^3$ and $n_B^0 = 10^6\,\mathrm{cm}^{-3}$ (note $k_1 = L_m(\mathrm{I})/L_{\mathrm{rad}}$, $k_2 = L_m^{\mathrm{MR}}(\mathrm{II})/L_{\mathrm{rad}}$ and $k_3 = L_m(\mathrm{I})/L_m^{\mathrm{MR}}(\mathrm{II})$)

Star	M_*	T_{eff}	t_9	N_1	N_2	L_{rad}	$L_m(\mathrm{I})$	$L_m^{\mathrm{MR}}(\mathrm{II})$	k_1	k_2	k_3
1	1.310	9110	2.60	7.9730e17	1.1987e19	2.2900e29	1.4689e30	3.7883e29	6.4014	1.6509	3.8775
2	1.330	11620	1.49	4.5230e17	3.8400e18	6.0100e29	8.5900e29	2.9477e29	1.4286	0.4902	2.9141
3	1.336	12080	1.71	5.1750e17	4.8720e18	7.0000e29	9.9170e29	3.2323e29	1.4164	0.4616	3.0682
4	1.351	29760	0.37	1.1120e17	2.5100e17	2.5601e31	2.1780e29	1.4507e29	0.0085	0.0057	1.5014
5	1.302	9420	2.59	7.9750e17	1.2292e19	2.6300e29	1.4514e30	3.6967e29	5.5100	1.4034	3.9261
6	1.319	34410	0.20	6.1000e16	8.8000e16	4.6495e31	1.1400e29	9.4760e28	0.0025	0.0020	1.2033
7	1.422	30200	0.35	1.0160e17	1.7200e17	2.6238e31	2.2060e29	1.6963e29	0.0084	0.0065	1.3005
8	1.314	9180	2.61	7.9870e17	1.1881e19	2.3600e29	1.4806e30	3.8388e29	6.2704	1.6258	3.8568
9	1.313	11150	2.18	6.6750e17	8.4730e18	5.1400e29	1.2354e30	3.4673e29	2.4028	0.6744	3.5630
10	1.329	10780	2.10	6.3780e17	7.4020e18	4.4600e29	1.2094e30	3.5503e29	2.7141	0.7967	3.4066
11	1.322	13480	1.72	5.2420e17	5.2090e18	1.0930e30	9.8360e29	3.1204e29	0.8996	0.2854	3.1523
12	1.344	10620	1.87	5.6370e17	5.5950e18	4.1700e29	1.0932e30	3.4701e29	2.6241	0.8329	3.1504
13	1.328	19470	1.08	3.2820e17	2.1010e18	4.7440e30	6.2140e29	2.4560e29	0.1310	0.0518	2.5300
14	1.307	19750	0.96	2.9480e17	1.8270e18	5.0770e30	5.4070e29	2.1718e29	0.1065	0.0428	2.4897
15	1.257	10940	3.34	1.0528e18	2.4012e19	4.9100e29	1.7859e30	3.7395e29	3.6407	0.7623	4.7758
16	1.326	21490	0.92	2.7980e17	1.5610e18	7.0480e30	5.2830e29	2.2364e29	0.0749	0.0317	2.3621
17	1.291	18450	1.06	3.2820e17	2.3550e18	3.8980e30	5.8730e29	2.1927e29	0.1507	0.0562	2.6785
18	1.304	10830	2.20	6.7670e17	8.9420e18	4.6000e29	1.2354e30	3.3984e29	2.6872	0.7392	3.6351
19	1.328	10160	2.11	6.4120e17	7.4990e18	3.5200e29	1.2140e30	3.5498e29	3.4509	1.0091	3.4199
20	1.320	13350	1.83	5.5830e17	5.9080e18	1.0530e30	1.0444e30	3.2108e29	0.9920	0.3050	3.2528
21	1.325	10660	2.21	6.7260e17	8.2870e18	4.2700e29	1.2677e30	3.6114e29	2.9691	0.8459	3.5102
22	1.318	14590	1.52	4.6420e17	4.1850e18	1.5040e30	8.6580e29	2.8832e29	0.5758	0.1918	3.0027
23	1.320	28030	0.43	1.3120e17	3.7700e17	2.0462e31	2.4540e29	1.4477e29	0.0120	0.0071	1.6952
24	1.303	16600	1.26	3.8780e17	3.1140e18	2.5390e30	7.0680e29	2.4942e29	0.2784	0.0982	2.8338
25	1.327	39910	0.12	3.6500e16	3.2000e16	8.3800e31	6.9000e28	7.3150e28	0.0008	0.0009	0.9429

luminosity of MMs that catalyze nuclear decay increases linearly with time until they become the main contribution to the total luminosity. One can even observe that for some of the oldest WDs, the luminosity may have passed its minimum, and some reheating may have occurred.

For example, for some low-mass WDs with a low lifetime (e.g., the O+Ne core WD J055631.17+130639.78 with $M_* = 1.207$, $t_9 = 3.33$ and $T_{\mathrm{eff}} = 8340$), the luminosity may increase linearly with time as the number of MMs captured increases from 1.6868×10^{30} erg to 1.6868×10^{32} erg at $T_6 = 0.1 \sim 10$ for model (I), but from 3.2192×10^{29} erg to 1.1422×10^{31} erg for model (II). For some high-mass C+O core WDs with a low lifetime, such as WD J190132.74 +145807.18 ($M_* = 1.422$, $t_9 = 0.35$, $T_{\mathrm{eff}} = 30200$), the luminosity may increase linearly with time as the number of MMs captured increases from 2.2060×10^{32} erg to 2.2060×10^{29} erg at $T_6 = 0.1 \sim 10$ for model (I), but from 1.6963×10^{29} erg to 6.0190×10^{30} erg for model (II).

Since we have neglected the effect on the mass–radius relation by the number of MMs captured by a WD, and only the mass–radius relation and the RC effect are considered in model (I), the luminosities can be overestimated, compared with model (II) (see Equations (8) and (11)). By considering the effect on the mass–radius relation by the number of MMs captured by a WD (see Equations (15), (18) and (19)), as well as the RC effect and the correction factor suppression, one sees that the calculations in model (II) agree well with the observations, and may be an improved estimation compared to model (I).

The annihilation of magnetic and antimagnetic monopoles can cause a significant reduction in the number of MMs and the catalytic luminosity of the monopole in WDs. Dicus et al. (1982) calculated the annihilation cross-sections of MMs and anti-MMs caused by two-body and three-body recombinations. Their results showed that this kind of annihilation has little effect on the flux and luminosity of MMs. The magnetic field may keep the MM and anti-MM distributions far enough apart that annihilation is negligible.

5. Conclusions

Proton decay catalyzed by MMs plays a key role in the evolution of burning WDs. Equations (15) and (16) show that if a WD contains enough monopoles, its radius will increase during the evolution. However, it may live much longer than the age of the universe, so the question of its energy source has been the focus of many astrophysical studies. In this work, we have investigated the problem of the energy source applied to 25 massive WDs. Some of our main results are summarized as

Table 5
The Comparisons Among Several Luminosities Due to the RC Effect for the C+O Core High-mass WD Model (Kilic et al. 2021) at Relatively High Temperature $T_6 = 10$, in which the parameters $1.257 \leqslant M_* \leqslant 1.422$, $m_{16} = 10$ GeV, $C = 7.037 \times 10^{-3}$, $\xi = 10^3$ and $n_B^0 = 10^6$ cm^{-3} (note $k_1 = L_m(\mathrm{I})/L_{\mathrm{rad}}$, $k_2 = L_m^{\mathrm{MR}}(\mathrm{II})/L_{\mathrm{rad}}$ and $k_3 = L_m(\mathrm{I})/L_m^{\mathrm{MR}}(\mathrm{II})$)

Star	M_*	T_{eff}	t_9	N_1	N_2	L_{rad}	L_m(I)	L_m^{MR}(II)	k_1	k_2	k_3
1	1.310	9110	2.60	7.9730e18	9.5220e20	2.2900e29	1.4689e32	1.3442e31	640.1393	58.5767	10.9282
2	1.330	11620	1.49	4.5230e18	3.0510e20	6.0100e29	8.5900e31	1.0459e31	142.8555	17.3939	8.2130
3	1.336	12080	1.71	5.1750e18	3.8700e20	7.0000e29	9.9170e31	1.1469e31	141.6359	16.3790	8.6474
4	1.351	29760	0.37	1.1120e18	1.9900e19	2.5601e31	2.1780e31	0.5147e30	0.8508	0.2011	4.2315
5	1.302	9420	2.59	7.9750e18	9.7640e20	2.6300e29	1.4514e32	1.3117e31	550.9982	49.7956	11.0652
6	1.319	34410	0.20	6.1000e17	7.0000e18	4.6495e31	1.1400e31	3.3620e30	0.2453	0.0723	3.3915
7	1.422	30200	0.35	1.0160e18	1.3700e19	2.6238e31	2.2060e31	6.0190e30	0.8408	0.2294	3.6652
8	1.314	9180	2.61	7.9870e18	9.4370e20	2.3600e29	1.4806e32	1.3621e31	627.0361	57.6847	10.8701
9	1.313	11150	2.18	6.6750e18	6.7310e20	5.1400e29	1.2354e32	1.2302e31	240.2805	23.9278	10.0419
10	1.329	10780	2.10	6.3780e18	5.8792e20	4.4600e29	1.2094e32	1.2597e31	271.4103	28.2686	9.6011
11	1.322	13480	1.72	5.2420e18	4.1380e20	1.0930e30	9.8360e31	1.1072e31	89.9630	10.1260	8.8843
12	1.344	10620	1.87	5.6370e18	4.4440e20	4.1700e29	1.0932e32	1.2312e31	262.4062	29.5538	8.8789
13	1.328	19470	1.08	3.2820e18	1.6690e20	4.7440e30	6.2140e31	8.7140e30	13.0975	1.8368	7.1305
14	1.307	19750	0.96	2.9480e18	1.4520e20	5.0770e30	5.4070e31	7.7060e30	10.6509	1.5179	7.0168
15	1.257	10940	3.34	1.0528e19	1.9074e21	4.9100e29	1.7859e32	1.3268e31	364.0657	27.0477	13.4601
16	1.326	21490	0.92	2.7980e18	1.2400e20	7.0480e30	5.2830e31	7.9350e30	7.4948	1.1258	6.6574
17	1.291	18450	1.06	3.2820e18	1.8710e20	3.8980e30	5.8730e31	7.7800e30	15.0662	1.9958	7.5492
18	1.304	10830	2.20	6.7670e18	7.1030e20	4.6000e29	1.2354e32	1.2058e31	268.7176	26.2286	10.2452
19	1.328	10160	2.11	6.4120e18	5.9560e20	3.5200e29	1.2140e32	1.2595e31	345.0927	35.8037	9.6385
20	1.320	13350	1.83	5.5830e18	4.6930e20	1.0530e30	1.0444e32	1.1392e31	99.1987	10.8204	9.1678
21	1.325	10660	2.21	6.7260e18	6.5830e20	4.2700e29	1.2677e32	1.2814e31	296.9117	30.0120	9.8931
22	1.318	14590	1.52	4.6420e18	3.3250e20	1.5040e30	8.6580e31	1.0230e31	57.5818	6.8041	8.4628
23	1.320	28030	0.43	1.3120e18	2.9900e19	2.0462e31	2.4540e31	5.1370e30	1.1994	0.2510	4.7777
24	1.303	16600	1.26	3.8780e18	2.4730e20	2.5390e30	7.0680e31	8.8500e30	27.8393	3.4857	7.9867
25	1.327	39910	0.12	3.6500e17	2.6000e18	8.3800e31	6.9000e30	2.5950e30	0.0823	0.0310	2.6575

follows: First, by considering the effect of temperature on the cross-section, thermonuclear reaction and mass–radius relation, we presented two MMs models (I, II) to discuss the issue of energy source. Second, we evaluated the number of MMs captured by WDs and compared the luminosities with observations. Finally, we discussed the effect of the correction factor on the cross-section in model (II) and the differences of luminosities between these two models.

We found that the luminosities of most of the O+Ne (or C +O) core massive WDs for models (I) and (II) agree well with the observations, and the difference is no more than one order magnitude at relatively low temperature (e.g., $T_6 = 0.1$). However, as the temperature increases (e.g., at $T_6 = 10$), the observations can be three and two orders of magnitude lower than those of model (I), and (II), respectively. We also have compared the results from the scaling factor k_3 of models (I) and (II). One can see that the maximum of the luminosities at low temperature (e.g., $T_6 = 0.1$) for model (I) is 5.2396 and 4.7758 times larger than those of model (II) for the O+Ne and the C+O core high-mass WDs, respectively (e.g., WD J055631.17+130639.78). However, the maximum of the luminosities at relatively high temperature (e.g., $T_6 = 10$) for model (I) is 14.7673 and 13.4601 times larger than those of model (II) for O+Ne and C+O core massive WDs, respectively (e.g., WD J055631.17+130639.78). Based on the above analysis and discussion, the monopole-catalyzed nucleon decay process could be preventing WDs from cooling down into a stellar graveyard by keeping them hot.

Acknowledgments

This work was supported in part by the National Natural Science Foundation of China (NSFC, grant Nos. 11965010 and 11565020), and the foundation for high-level talents program of Hainan basic and applied basic research program (natural science) under grant 2019RC239, and the Natural Science Foundation of Hainan Province under grants 118MS071 and 114012, the Counterpart Foundation of Sanya under grants 2016PT43 and 2019PT76, the Special Foundation of Science and Technology Cooperation for Advanced Academy and Regional of Sanya under grant 2016YD28, and the Scientific Research Starting Foundation for 515 Talented Project of Hainan Tropical Ocean University under grant RHDRC201701.

References

Ahlen, S., & Kinoshita, K. 1982, Phys. Rev. D., 26, 2347
Arafune, J., & Fukugita, M. 1983, Phys. Rev. Lett., 50, 1901
Avakian, R. M. 1972, CoBAO, 44, 115

Bildsten, L., & Hall, D. M. 2001, ApJL, 549, 219
Callan, C. G. 1983, Nucl. Phys., 212, 391
Caplan, M. E., Horowitz, C. J., & Cumming, A. 2020, ApJL, 902L, 44C
Cheng, S. H., Cummings, J. D., & Mnard, B. 2019, ApJ, 886, 100
Cox, J. P., & Giuli, R. T. 1968, Principles of Stellar Structure (New York: Gordon and Breach)
Detrixhe, M., Besson, D., Gorham, P. W., et al. 2011, Phys. Rev. D., 83, 3513
Deloye, C. J., & Bildsten, L. 2002, ApJ, 580, 1077
Deng, Z. L., Gao, Z. F., Li, X. D., et al. 2020, Astrophys. J., 892, 4
Deng, Z. L., Li, X. D., Gao, Z. F., et al. 2021, Astrophys. J., 909, 174
Dicus, D. A., Page, D. N., & Teplitz, V. L. 1982, Phys. Rev. D., 26, 1306
Dong, A. J., Gao, Z. F., et al. 2023, Acta Phys. Sin., 72, 030502
Frank, M., Antoshkin, A., Dukes, C., et al. 2019, ICRC, 36, 888
Freese, K. 1984, ApJ, 286, 216
Freese, K., & Krasteva, E. 1999, Phys. Rev. D., 59, 063007
Fujii, T., & Pierre, A. C. 2015, ICRC, 34, 319
Fu, G. Z., Xing, C. C., & Na, W. 2020, EPJC, 80, 582
Gao, Z. F., Li, X. D., Wang, N., et al. 2016, MNRAS, 456, 55
Gao, Z. F., Wang, N., Shan, H., et al. 2017, ApJ, 849, 19
Gao, Z. F., Omar, N., Shi, X. C., et al. 2019, Astron. Nachr., 340, 1030
Gao, Z. F., Wang, H., Zhao, X. J., & Yang, X. F. 2023, Astron. Nachr., 344, e20220112
G't, H. 1974, NuPhB, 79, 276
Garcła-Berro, E., Althaus, L. G., Córsico, A. H., et al. 2008, ApJ, 677, 473
Izawa, M. 1986, PThPh, 75, 556
Kain, B. 2019, Phys. Rev. D., 100, 3003
Kilic, M., Bergeron, P., Blouin, S., et al. 2021, MNRAS, 503, 5397
Kolb, E., & Turner, M. S. 1984, ApJ, 286, 702
Liu, J. J. 2013, MNRAS, 433, 1108
Liu, J. J. 2014, MNRAS, 438, 930
Liu, J. J., & Gu, W. M. 2016a, ApJS, 224, 29
Liu, J. J. 2016b, Ap&SS., 361, 246
Liu, J. J., & Liu, D. M. 2016c, RAA, 16, 83
Liu, J. J. 2016d, RAA, 16, 174
Liu, J. J., et al. 2017a, ChPhC, 41, 95101
Liu, J. J., et al. 2017b, RAA, 17, 107
Liu, J. J., & Liu, D. M. 2017c, ChPhC, 41, 5102
Liu, J. J., & Liu, D. M. 2018a, EPJC, 78, 84
Liu, J. J., & Liu, D. M. 2018b, RAA, 18, 8
Liu, J. J., Hao, L. H., & Liu, D. M. 2023a, ChPhC, 47, 084106
Liu, J. J., Liu, D. M., & Pneg, Q. H. 2023b, IJMPD., 32, 2350045
Liu, J. J., & Liu, D. M. 2023c, Journal of High Energy Astrophysics., 39, 70
Liu, J. J., & Liu, D. M. 2023d, MPLA, 38, 2350084
Li, X. H., Gao, Z. F., Li, X. D., et al. 2016, IJMPD, 25, 25165000
Li, B. P., & Gao, Z. F. 2023, Astron. Nachr., 344, e20220111
Li, B. P., Ma, W. Q., & Gao, Z. F. 2023, Astron. Nachr., e20230167
Lobato, R. V., Malheiro, M., & Coelho, J. G. 2018, in The Fourteenth Marcel Grossmann Meeting On Recent Developments in Theoretical and Experimental General Relativity, Astrophysics, and Relativistic Field Theories (Rome: World Scientific Publishing Co.), 4313
Ma, Z. Q., & Tang, J. F. 1983, PhLB, 153, 59
Malkus, W. V. R. 1951, Phys. Rev., 83, 889
Mestel, L. 1952, MNRAS, 112, 583
Parker, E. 1970, ApJ, 160, 383
Peng, Q. H., Lie, Z. Y., & Wang, D. Y. 1985, Scientia Sinica (Serries A), 28, 970
Peng, Q. H., Liu, J. J., & Ma, Z. Q. 2017, NewA, 57, 59
Peng, Q. H., Liu, J. J., & Chou, C. K. 2020, MPLA, 35, 2050030
Peng, Q. H., & Liu, J. J. 2023, J. High Energy Physics, Gravitation and Cosmology, 9, 438
Polyakov, A. M. 1974, JETP. Lett., 20, 194
Rajantie, A. 2012, RSPTA, 370, 5705
Rubakov, V. 1981, JETP Lett., 33, 644
Wang, H., Gao, Z. F., Jia, H. Y., et al. 2020, Universe, 6, 63
Yan, F. Z., Gao, Z. F., Yang, W. S., et al. 2021, Astron. Nachr., 342, 249
Zhu, C., Gao, Z. F., Li, X. D., et al. 2016, MPLA, 31, 1650070